Available online at www.sciencedirect.com
ScienceDirect
Journal of Power Sources 172 (2007) 155–162
JOURNAL OF POWER SOURCES
www.elsevier.com/locate/jpowsour

Transient phenomena in a PEMFC during the start-up of gas feeding observed with a 97-fold segmented cell

Zyun Siroma*, Naoko Fujiwara, Tsutomu Ioroi, Shin-ichi Yamazaki, Hiroshi Senoh, Kazuaki Yasuda, Kazumi Tanimoto

Research Institute for Ubiquitous Energy Devices, National Institute of Advanced Industrial Science and Technology (AIST), Ikeda, Osaka 563-8577, Japan

Received 27 June 2007; received in revised form 30 July 2007; accepted 31 July 2007
Available online 6 August 2007

Abstract

To measure local phenomena in a PEMFC during a transitional state induced by changing of the feeding gas, a segmented cell was fabricated and the local current and local potential distribution were measured under open-circuit conditions. The anode or cathode was divided into 97 segments of 1.5 mm each. A change in the anode gas from nitrogen or oxygen to hydrogen induced momentary internal currents among the segments. The potential distribution in the electrolyte was observed simultaneously using three quasi-reference electrodes located locally. The results supported the reverse-current decay mechanism, which is known to be a mechanism of cathode degradation. Furthermore, internal currents were observed when the cathode gas was changed from nitrogen to oxygen. While the cathode was not subjected to a harmful potential, a large potential distribution was induced in the anode.

Keywords: Proton exchange membrane fuel cell; Degradation mechanism; Current distribution; Segmented cell

1. Introduction

Before proton exchange membrane fuel cells (PEMFCs) can be commercialized, the short lifetime of the membrane electrode assembly (MEA) must be overcome. To achieve a long life of up to several tens of thousands of hours, accelerated degradation tests are required. However, there is so far no standard accelerated test for degradation because the mechanisms of degradation phenomena are not yet clear. Aside from the mechanisms, there are several conditions or procedures that are phenomenologically known to accelerate degradation, such as operation under low humidity [1–4], retention under an open-circuit condition [5–7], potential cycling of the cathode [5,8–10], and cycling of start-up and shut-down [11]. It is important to elucidate the phenomena and mechanisms of such degradative conditions.

Oxygen- and hydrogen-rich regions coexist in the anode during start-up (fuel introduction) and shut-down (air purge). A mechanism of degradation under such transient conditions, called the "reverse-current decay mechanism", has been proposed [12,13]. A similar mechanism was also proposed and examined by Farooque et al. [14] in the case of phosphoric acid fuel cells (PAFCs) when there is air leakage to the anode. In their experiment, oxygen was intentionally introduced to the anode to simulate cross-leaking from the cathode. According to this mechanism, the existence of oxygen in a local region in the anode leads to an abnormally high potential at the cathode in that region, which in turn leads to corrosion locally. No previous reports have directly substantiated this mechanism, i.e., a local current distribution and local potential distribution in a cell during a transient condition caused by a change in gas feeding. In the present study, we examined the transient condition; we changed the anode gas from oxygen to hydrogen, and from nitrogen to hydrogen, and also changed the cathode gas from nitrogen to oxygen. Since the geometrical distribution of local currents during a transient condition was uncertain before

* Corresponding author. Tel.: +81 72 751 9653; fax: +81 72 751 9629.
E-mail address: siroma.z@aist.go.jp (Z. Siroma).

0378-7753/$ – see front matter © 2007 Elsevier B.V. All rights reserved.
doi:10.1016/j.jpowsour.2007.07.062

the experiment, we made a segmented cell with as many small segments as possible.

2. Experimental

A PEMFC with a segmented current collector on one side and a continuous current collector on the other side of a membrane-electrode assembly (MEA) was fabricated. The segmented side was used for the anode or the cathode depending on the experiment. Fig. 1 shows a schematic of the segmented cell when the segmented side was used for the anode. The segmented current collector consists of 97 segments arranged as a triangular lattice in a circular area of Ø 2.5 cm. For the counter side (cathode side in this case), a normal flow-field plate made of titanium with straight channels and ribs 1 mm wide was used. The gas diffusion electrode (catalyst layer and gas diffusion layer) on the segmented side was also divided into 97 sections with the same pattern as the segmented current collector shown in Fig. 1(b) to electronically isolate them from each other. Consequently, the active area of the anode was 34% of the Ø 2.5 cm area. A commercially available gas diffusion electrode (0.5 mg Pt cm^{-2}, E-TEK) was used for both the anode and cathode. The MEA was fabricated by hot-pressing of 97 pieces of anode, electrolyte membrane (Nafion® 117), and cathode.

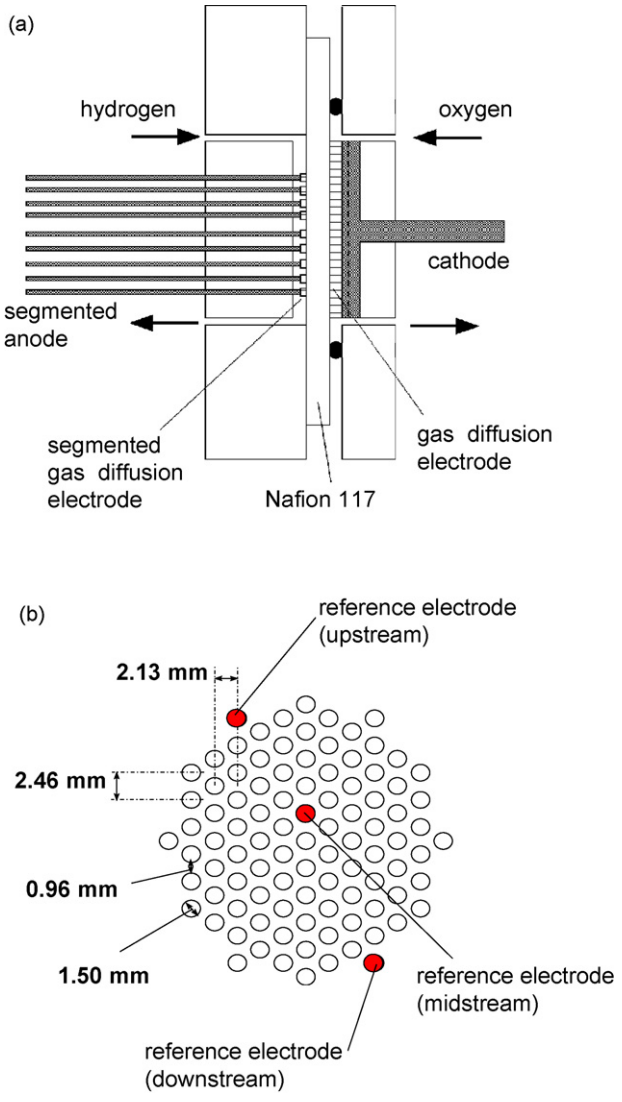

Fig. 1. (a) Schematic of a Ø 2.5 cm cell with a 97-fold segmented anode and (b) layout of the segments (both current collector and gas diffusion electrode).

Segments of the anode current collector were all connected to each other by a 100ch zero-shunt current/voltage converter (IVC-100MS, Ekurea) to obtain the current value without any voltage loss. Since the cell was externally under open-circuit conditions in every experiment, the cathode current collector was left unconnected. The output of the current/voltage converter was recorded using a data logger (8422, Hioki) every 0.2 s. Local currents of same and opposite direction compared with the normal operation of the fuel cell are called "forward current" and "backward current", and expressed with plus and minus signs, respectively. The segmented cell and humidifiers for the feeding gases were kept at 80 °C. Gas feeding for both the anode and cathode was performed at 50 sccm under atmospheric pressure. Among the segments, three segments were selected for use as reference electrodes at upstream, midstream, and downstream, respectively. These three segments were disconnected from the current/voltage converter and their potentials were monitored directly using the data logger (input impedance is 1 MΩ). Each of these segments acts as a reversible hydrogen electrode (RHE). When oxygen is fed to the segmented side, it is expected to be a quasi-reference electrode which shows the open-circuit potential of the cathode of a PEMFC (ca. 1.0 V vs. RHE). Despite the accuracy and stability of these reference electrodes, there is some question regarding about the interpretation of values obtained by reference electrodes, as pointed out by He et al. [15]. However, although these reference electrodes are tentative and may not show the potential exactly, any potential difference that may arise among them can be interpreted as a potential difference in the electrolyte membrane in the in-plane direction.

To substantiate the reverse-current decay mechanism, a change in the anode gas from 5% oxygen (diluted with nitrogen) to hydrogen was examined. Furthermore, to investigate the phenomena at start-up from an initial stage with a nitrogen purge in detail, two series of experiments consisting of changes in anode and cathode gas-feeding were performed. All sequences are summarized in Fig. 2. The latter two procedures differ according to the order in which the active gases are introduced. This means that we can examine the effects of the atmosphere of the counter electrode; for example, the introduction of hydrogen into the

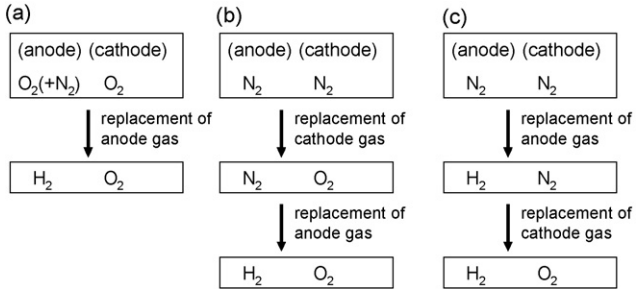

Fig. 2. Three procedures for changing feeding gases.

anode in sequences (b) and (c) is accompanied by feeding the counter electrode oxygen and nitrogen, respectively.

Generally, a period of a transient phenomenon induced by changing of the feeding gas depends on the sharpness of the gas boundary made in the feeding line; if mixing of two gases proceeds before reaching to the inlet of the cell, the phenomenon becomes dull and takes a longer time. Although the periods of the transient phenomena in our results varied with each run, they were within several seconds in every case.

3. Results

3.1. Change in the anode gas from 5% oxygen to hydrogen

Fig. 3 shows the change in the cell voltage and current of each segment when the anode gas was changed from 5% oxygen (diluted with nitrogen) to hydrogen. The segmented side was the anode. The abscissa values (time from the beginning of this run of the experiment) are not important in themselves but will be referred to in Fig. 4. A change in the gas in the anode induced an increase in the cell voltage and a temporary current between the segments (their sum was always zero). Fig. 4 shows the changes in the geometrical current distribution of 97 segments during this transient phenomenon, which allows us to image the event as an animation. First, the uppermost segments showed comparatively large forward current, which was compensated by the backward current shared by other segments. Next, the boundary between the areas where the current flows forward and backward, respectively, shifted downward along with the gas flow.

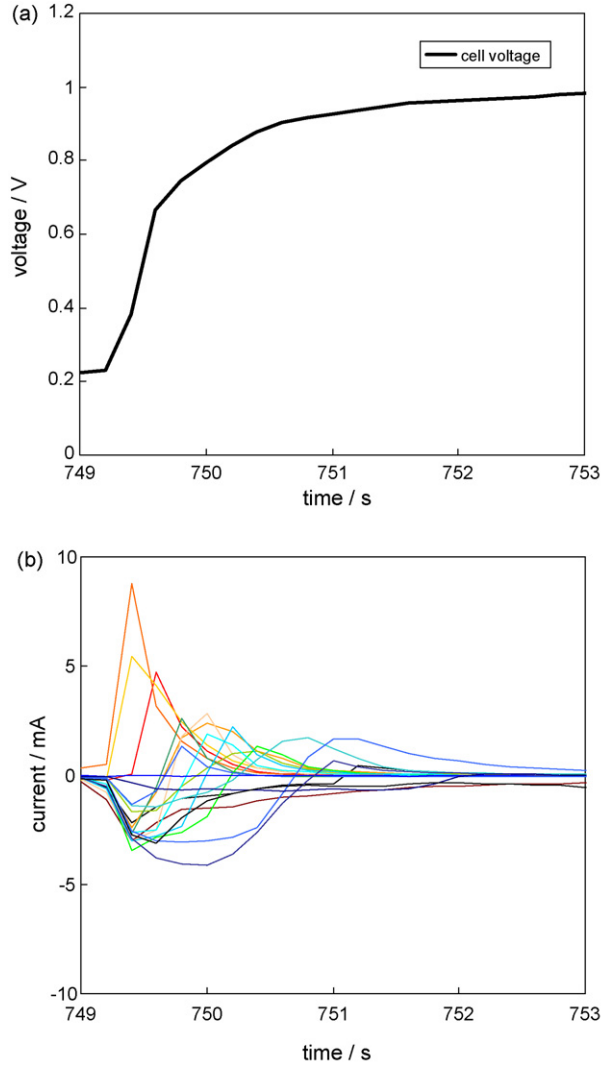

Fig. 3. Changes in the (a) voltage and (b) current of each segment of the anode-segmented cell when the anode gas was changed from O_2 (5%) to H_2. To avoid congestion in the plot of the current values, 20 values were selected (one for every five data points).

Although Fig. 3(b) was drawn using 20 selected segments, it is still hard to read qualitatively. To facilitate understanding, several segments in three typical regions (upstream, midstream, and downstream) were examined as shown in Fig. 5(a) and the average current value in each region was calculated as shown in Fig. 5(b). Throughout the event, the currents in the upstream and downstream segments were positive and negative, respectively. The current in the midstream segments was initially negative, like downstream, then become positive, like upstream.

Fig. 6 shows the results of the same experiment as described above but where the segmented side was the cathode. In this experiment, three reference electrodes were used during the transient phenomena because the atmosphere around them was constantly oxygen. Therefore, not only the cell voltage but also the potentials of the anode and cathode versus each of the three reference electrodes, i.e., local electrode potentials, can be estimated as shown in Fig. 6(a). Each local anode potential (i.e., anode potential versus each local potential of the electrolyte) decreased from upstream to downstream in the order of the direction of gas flow. As a result, the local cathode potentials temporarily showed high values, except upstream. This is due to the fact that all parts always share a common cell voltage (potential difference of the anode and cathode), as theoretically predicted by Reiser et al. [12]. The geometrical distribution of the current, which is not shown, was qualitatively the same as the result shown in Fig. 4.

3.2. Change in the cathode gas from nitrogen to oxygen, followed by a change in the anode gas from nitrogen to hydrogen

According to the procedure shown in Fig. 2(b), a cell that had been deactivated by a nitrogen purge was started by sequential replacement of the cathode and anode gas by oxygen and hydrogen, respectively. Fig. 7 shows the results when the segmented side was used as the cathode. In this case, the local reference electrodes worked during the latter transition ($t = 494$ s), since the atmosphere around them became oxygen after the former transition ($t = 198$ s). The former transition caused a small change in the cell voltage and almost no local current. On the other hand, despite the inert atmosphere in the anode downstream, a phenomenon similar to that shown in Fig. 6 was observed in the latter transition.

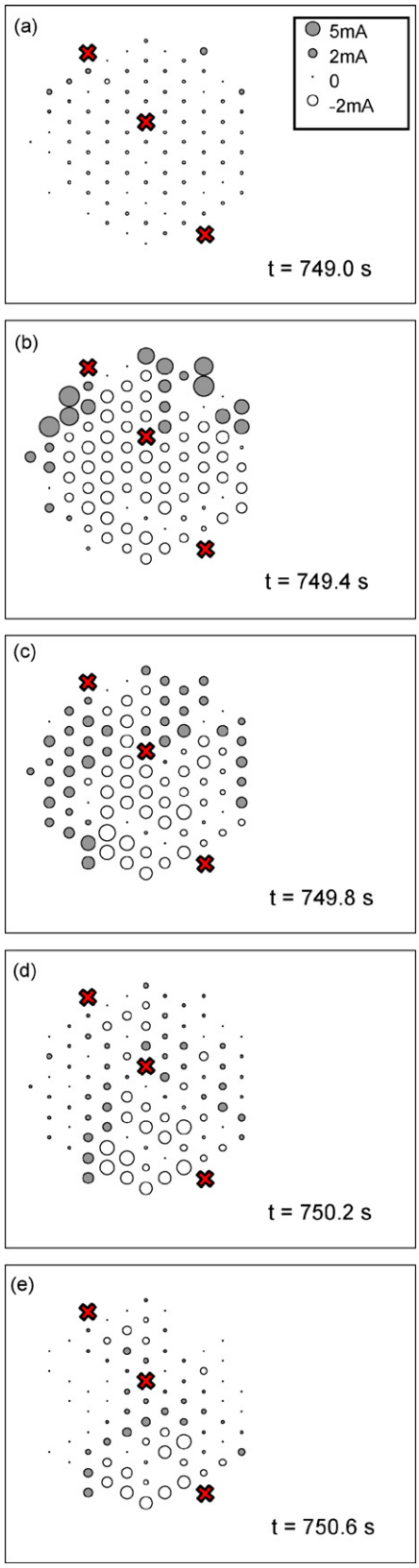

Fig. 4. Geometrical distribution of the current during the change shown in Fig. 3. Gas flowed from the top to the bottom. The size of each circle indicates the magnitude of the current. White circles indicate backward current compared with the normal current of the fuel cell. Three crosses indicate the positions of local reference electrodes.

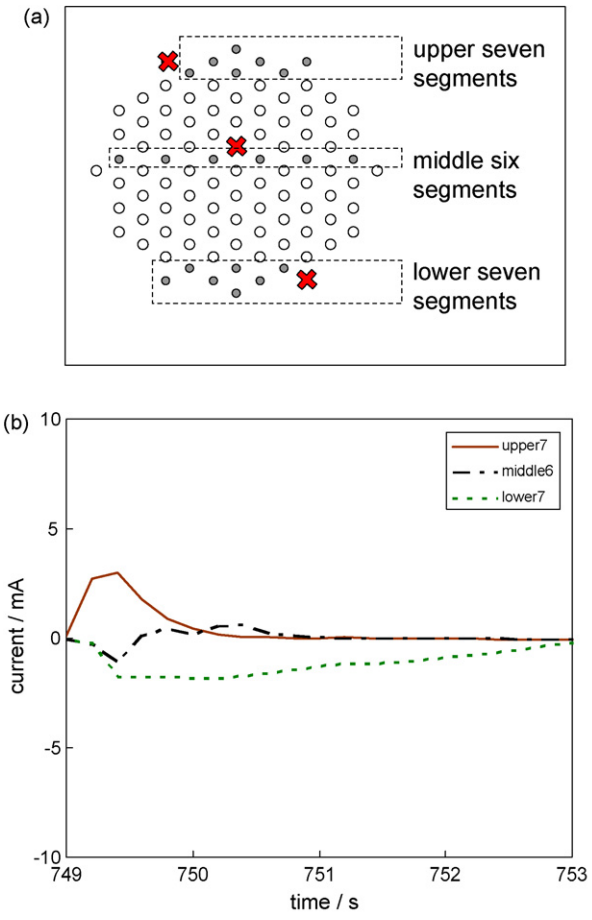

Fig. 5. (a) Layout of three regions and (b) average current values of the segments in each region calculated from the data shown in Fig. 3(b).

3.3. Change in the anode gas from nitrogen to hydrogen, followed by a change in the cathode gas from nitrogen to oxygen

According to the procedure shown in Fig. 2(c), a cell that had been deactivated by a nitrogen purge was started by sequential replacement of the anode and cathode gas by hydrogen and oxygen, respectively. Fig. 8 shows the results when the segmented side was used as the anode. In this case, the local reference electrodes worked during the latter transition ($t = 776$ s), since the atmosphere around them became hydrogen after the former transition ($t = 353$ s). The former transition caused a change in the cell voltage accompanied by slight local current (note the magnitude of the ordinate in Fig. 8(c)). The local anode and cathode potentials during the latter transition shown in Fig. 8(b) were in complete contrast to the results shown in Figs. 6(a) or 7(b): each local cathode potential increased from upstream to downstream in the order of the direction of gas flow, and local anode potentials showed a temporary low value, except upstream. Fig. 9 shows the geometrical current distribution during the latter transition phenomenon. The magnitude of the local current shown in Figs. 8(d) and 9 is as large as those in any of the other transitions.

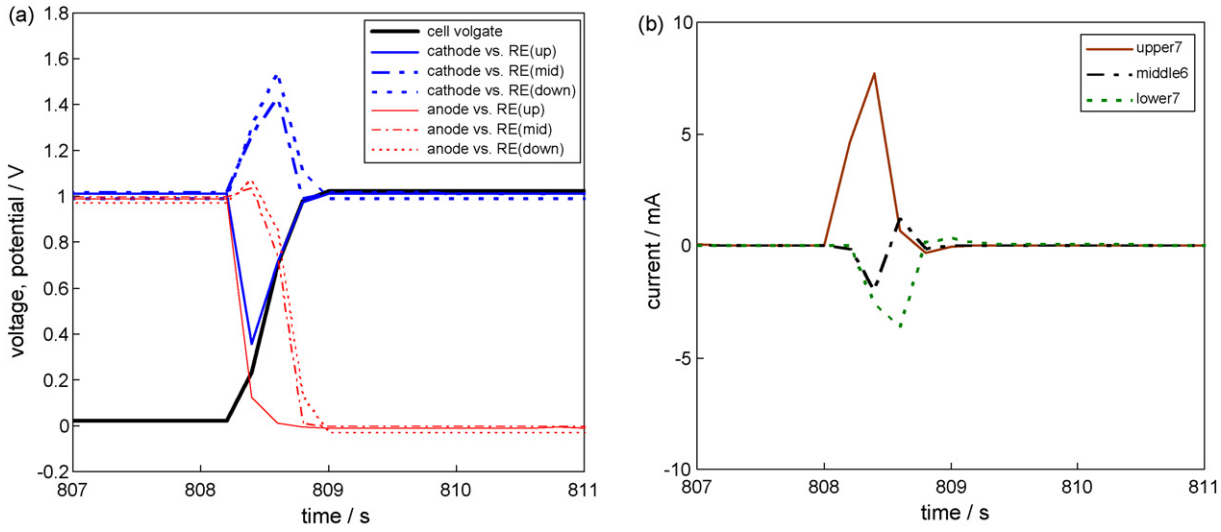

Fig. 6. Changes in the (a) voltage and local potentials and (b) average current in three regions of the cathode-segmented cell when the anode gas was changed from O_2 (5%) to H_2.

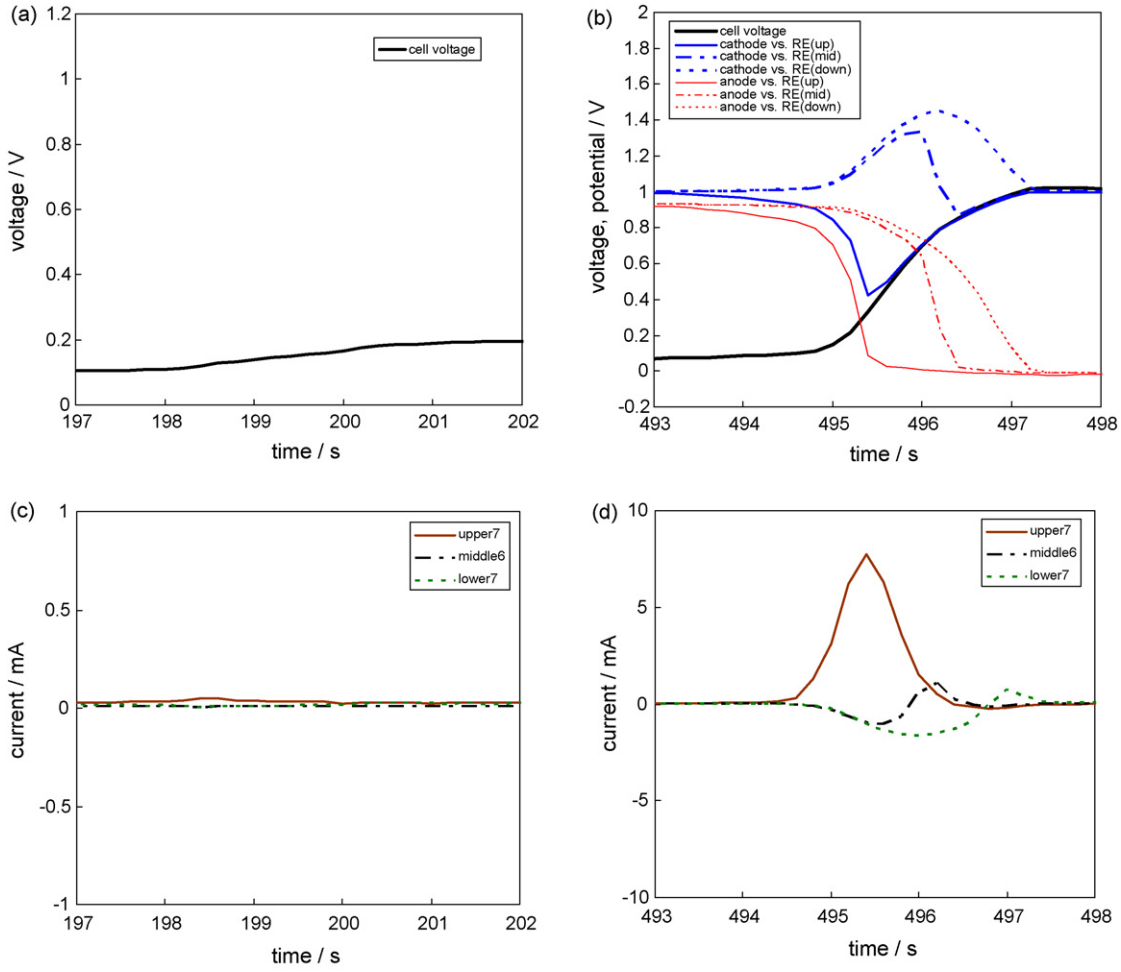

Fig. 7. Changes in the (a, b) voltage and local potentials of the anode and cathode and (c, d) average current in three regions of the cathode-segmented cell when the cathode gas was changed from N_2 to O_2 at $t = 198$ s, followed by a change in the anode gas from N_2 to H_2 at $t = 494$ s.

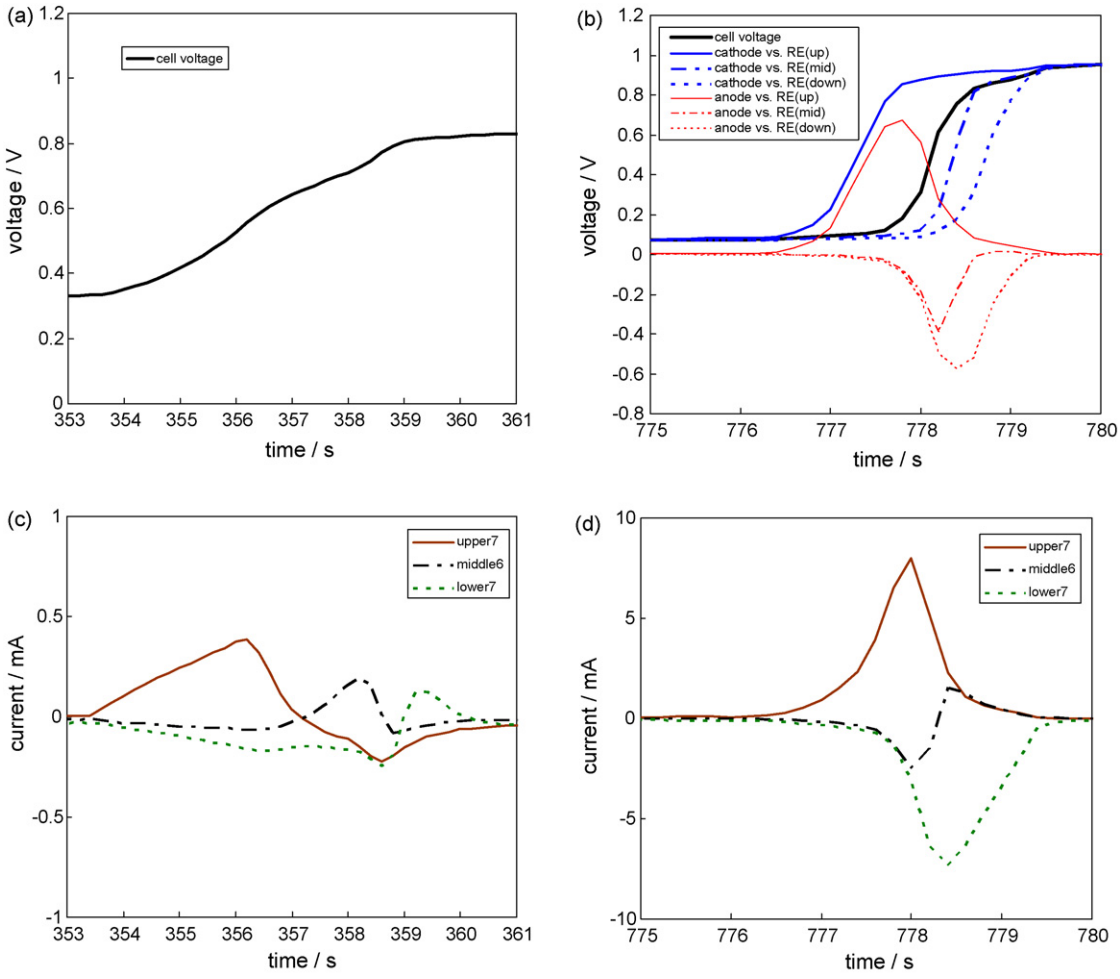

Fig. 8. Changes in the (a, b) voltage and local potentials of the anode and cathode and (c, d) average current in three regions of the anode-segmented cell when the anode gas was changed from N_2 to H_2 at $t = 353$ s, followed by a change in the cathode gas from N_2 to O_2 at $t = 776$ s.

4. Discussion

The reverse-current decay mechanism supposes backward current compared with the normal current in the fuel cell in the region where oxygen exists in the anode. In such a region, oxygen exists at both sides of the electrolyte, which constitutes an oxygen pump. Therefore, the whole cell can be assumed to be a serial connection of two local cells, i.e., a fuel cell representing the "normal" region and an oxygen pump representing the "abnormal" region, with a common cell voltage. An oxygen reduction reaction (ORR) and oxygen evolution reaction (OER) occur in the negative and positive electrodes (cathode and anode in this localized cell) of the oxygen pump, respectively. The local potential of the positive electrode is unexpectedly high and is accompanied by the corrosion of carbon material. The potential profile of such an inhomogeneous cell is illustrated schematically in Fig. 10(a).

In the normal region, the potential of the cathode against the electrolyte is determined by subtracting the overvoltage of the ORR from the thermodynamic potential of the H_2O/O_2 redox couple (1.23 V). The potential of the anode against the electrolyte is determined by adding the overvoltage of the hydrogen oxidation reaction (HOR) to the thermodynamic potential of the H_2/H^+ redox couple (0 V). The potential incline in the electrolyte, or *iR* drop, is determined by the conductivity and current value. These three values decide the cell voltage of the normal region. In the abnormal region, the potential of the positive electrode against the electrolyte is determined by adding the overvoltage of the OER to 1.23 V. (Carbon corrosion may be a dominant reaction depending on the potential. Here we assumed it was a side reaction that accompanied OER to simplify the explanation.) The potential of the negative electrode against the electrolyte is determined by subtracting the overvoltage of the ORR from 1.23 V. The *iR* drop has an opposite sign because the current direction is opposite. Let us consider the theoretical prediction if hydrogen exists in the cathode locally, as shown in Fig. 10(b), for the convenience of the later discussion. In contrast to the case shown in Fig. 10(a), the abnormal region acts as a hydrogen pump. The potential of the positive electrode against the electrolyte is determined by adding the overvoltage of the HOR to 0 V. The potential of the negative electrode against the electrolyte is determined by subtracting the overvoltage of the hydrogen evolution reaction (HER) from 0 V, which is an unexpectedly low value (but not harmful). Ye et al. [16,17] reported

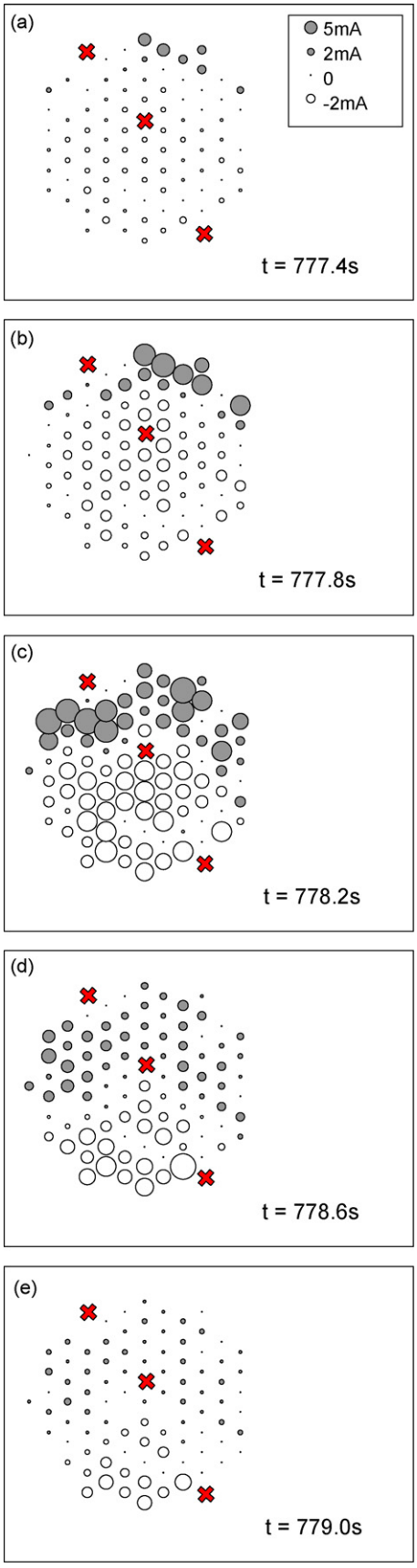

Fig. 9. Geometrical distribution of the current during the latter change shown in Fig. 8(b, d).

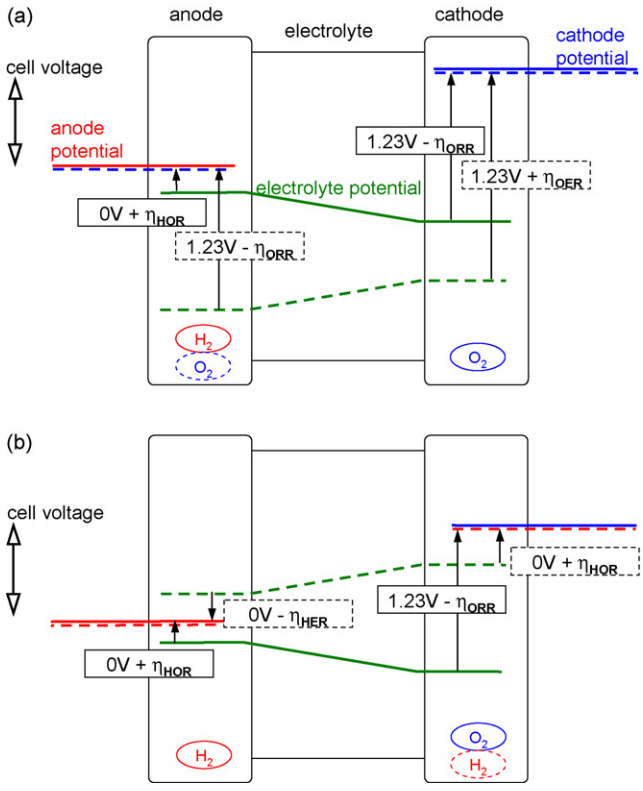

Fig. 10. Schematic of the potential profiles in a PEMFC when (a) there is oxygen in the anode locally and (b) there is hydrogen in the cathode locally. Dotted lines indicate the "abnormal" region in which oxygen exists in the anode or hydrogen exists in the cathode.

hydrogen evolution from the anode of a direct methanol fuel cell (DMFC) under air-starvation conditions. In this case, the existence of cross-leaked methanol in the cathode is assumed to be a source of the reverse current. Besides the fuel, the principle is identical to what is shown in Fig. 10(b).

Our results shown in Figs. 3–6 are consistent with the reverse-current decay mechanism illustrated in Fig. 10(a). Internal current was observed not only when the segmented side was used as an anode (Figs. 3–5) but also when the segmented side was used as a cathode (Fig. 6). This means that the potential difference which arises due to a difference in atmosphere makes an internal local current by way of the counter electrode. This is an important feature of reverse-current. The reverse-current decay mechanism may be similar to the idea of a "local galvanic cell" in the field of metal corrosion, albeit the local galvanic cell is composed of one electrode | electrolyte boundary with no additional electrode. Fig. 10 implies that there is a large potential difference in the electrolyte between the normal and abnormal regions. Such a large potential difference can exist because the electrolyte membrane is very thin and has little ionic conductivity in the in-plane direction. If the electrolyte membrane were so thick that ionic current easily flowed in the in-plane direction in a cell, the resulting condition would be like a local galvanic cell and the effect would not extend to the counter electrode.

A similar result was obtained when the preceding gas in the anode did not contain oxygen, as shown in Fig. 7(b and d). However, some reactions should be assumed to explain the source

of the reverse current. There are two candidates for the source of the reverse current. One is the reduction of the cross-leaked oxygen from the cathode. There is a slight difference in voltage between the end of the former transition ($t = 202$ s) and the beginning of the latter transition ($t = 493$ s). This is caused by the penetration of oxygen from the cathode to the anode during this period. Therefore, there was a small amount of oxygen in the anode before the latter transition. In practice, degradation by the reverse-current decay mechanism has been reported to occur not only when oxygen is introduced in the anode [18] but also when the supply of hydrogen is suppressed [19]. Cross-leaked oxygen was assumed to contribute to degradation in the latter case. The other candidate for the reverse current in our result is charging of the electrical double layer. In contrast to steady-state phenomena, a transient current does not necessarily require a faradaic process. In fact, a small amount of current was observed in the former transition in the experiment shown in Fig. 8(c). In this case, the preceding atmospheres for both the anode and cathode were inert, so the current downstream should be nonfaradaic. Therefore, the description of the reverse-current decay mechanism can be extended from Fig. 10(a) in the case of a transient phenomenon; reactions at the negative and positive electrodes in the abnormal region are not limited to oxygen reduction and oxygen evolution, but include charging of the electrical double layer. The magnitude of the double layer capacitance can be estimated by cyclic voltammetry in an inert condition. Our segmented cell shows ca. 1 mF per segment. Therefore, if a potential change of 1 V occurs during 1 s, a charging current on the order of 1 mA is expected. It is reasonable to expect double layer charging to play a role in the internal current.

Our results shown in Figs. 8(b, d) and 9 are consistent with the mechanism illustrated in Fig. 10(b). There is no preceding hydrogen in the cathode in this experiment. Again, there are at least two possible explanations for the source of the reverse current: oxidation of cross-leaked hydrogen from the anode and charging of the electrical double layer. Therefore, strictly speaking, the description shown in Fig. 10(b) should also contain charging of the electrical double layer in addition to faradaic processes in the abnormal region.

Although the local potential of the cathode did not exhibit a harmful value at any position, a comparatively large overpotential of the anode was observed upstream, as shown in Fig. 8(b). (Usually the magnitude of this overpotential may be not necessarily so large, since at this stage the mechanism of such a large polarization is not clear.) This implies that the preferred degradation of the anode upstream may be caused by repetitive changes in the cathode feeding gas if the anode catalyst contains ruthenium, which tends to dissolve under a higher potential.

Our technique using a segmented cell with many small segments was shown to be effective for mapping the internal current distribution. Furthermore, the use of several reference electrodes in a cell was effective for elucidating the mechanism of the internal current. These techniques may become powerful tools for investigations not only during transient conditions, but also under steady-state operation, including local malfunctions and small spontaneous fluctuations of the reaction.

5. Conclusions

Transition phenomena induced by changes in the feeding gas were observed using a 97-fold segmented cell with three reference electrodes set at upstream, midstream, and downstream. A change in the anode gas from oxygen (diluted with nitrogen) to hydrogen induced internal currents among the segments and transient local electrode potentials. In accordance with the reverse-current decay mechanism, the local cathode potential downstream became abnormally high, which should lead to carbon corrosion. A change in the anode gas from nitrogen to hydrogen induced similar phenomena. The presence of cross-leaked oxygen in the anode and charging of the electrical double layer are assumed to be the source of the reverse current. In contrast, a change in the cathode gas from nitrogen to oxygen induced phenomena that were in contrast to the previous experiments: the local anode potential downstream became abnormally low, which should lead to hydrogen evolution.

Acknowledgements

This work was financially supported by the New Energy and Industrial Technology Development Organization (NEDO) as part of the Research and Development of Polymer Electrolyte Fuel Cell Technology Project directed by the Ministry of Economy, Trade and Industry (METI), Japan. The authors thank Mr. Akihiro Nishikawa and Mr. Yoshimasa Hosoi for their help with the experimental set-up and data collection.

References

[1] E. Endoh, S. Terazono, H. Widjaja, Y. Takimoto, Electrochem. Solid-State Lett. 7 (2004) A209.
[2] S.D. Knights, K.M. Colbow, J. St-Pierre, D.P. Wilkinson, J. Power Sources 127 (2004) 127.
[3] J. Yu, T. Matsuura, Y. Yoshikawa, M.N. Islam, M. Hori, Phys. Chem. Chem. Phys. 7 (2005) 373.
[4] M. Inaba, H. Yamada, R. Umebayashi, M. Sugishita, A. Tasaka, Electrochemistry 75 (2007) 207.
[5] P.J. Ferreira, G.J. la O', Y. Shao-Horn, D. Morgan, R. Makharia, S. Kocha, H.A. Gasteiger, J. Electrochem. Soc. 152 (2005) A2256.
[6] M. Inaba, T. Kinumoto, M. Kiriake, R. Umebayashi, A. Tasaka, Z. Ogumi, Electrochim. Acta 51 (2006) 5746.
[7] T. Akita, A. Taniguchi, J. Maekawa, Z. Siroma, K. Tanaka, M. Kohyama, K. Yasuda, J. Power Sources 159 (2006) 461.
[8] P. Yu, M. Pemberton, P. Plasse, J. Power Sources 144 (2005) 11.
[9] K. Yasuda, A. Taniguchi, T. Akita, T. Ioroi, Z. Siroma, Phys. Chem. Chem. Phys. 8 (2006) 746.
[10] D. Liu, S. Case, J. Power Sources 162 (2006) 521.
[11] H. Chizawa, Y. Ogami, H. Naka, A. Matsunaga, N. Aoki, T. Aoki, ECS Trans. 3 (2006) 645.
[12] C.A. Reiser, L. Bregoli, T.W. Patterson, J.S. Yi, J.D. Yang, M.L. Perry, T.D. Jarvi, Electrochem. Solid-State Lett. 8 (2005) A273.
[13] J.P. Meyers, R.M. Darling, J. Electrochem. Soc. 153 (2006) A1432.
[14] M. Farooque, A. Kush, L. Christner, J. Electrochem. Soc. 137 (1990) 2025.
[15] W. He, T.V. Nguyen, J. Electrochem. Soc. 151 (2004) A185.
[16] Q. Ye, T.S. Zhao, Electrochem. Solid-State Lett. 8 (2005) A211.
[17] Q. Ye, T.S. Zhao, J.G. Liu, Electrochem. Solid-State Lett. 8 (2005) A549.
[18] H. Tang, Z. Qi, M. Ramani, J.F. Elter, J. Power Sources 158 (2006) 1306.
[19] T.W. Patterson, R.M. Darling, Electrochem. Solid-State Lett. 9 (2006) A183.